Supporting information

Hydrogen spillover-driven selective hydrogenation of nitrobenzoic acid to aminobenzoic acid over a ZIF-8/$Cu(OH)_2$ heterostructure

Meiqing Cai, Wenbiao Wang, Junhua Li, Ximin Zhang, Hui Qian, Xiaohui Xu, Xinjie Tian, Youbing Huang and Jun-Ling Song*

International Joint Research Center for Photoresponsive Molecules and Materials,School of Chemical and Material Engineering, Jiangnan University, Lihu Street 1800, Wuxi 214122, China

* Email addresses: (Jun-Ling Song) jlsong@jiangnan.edu.cn

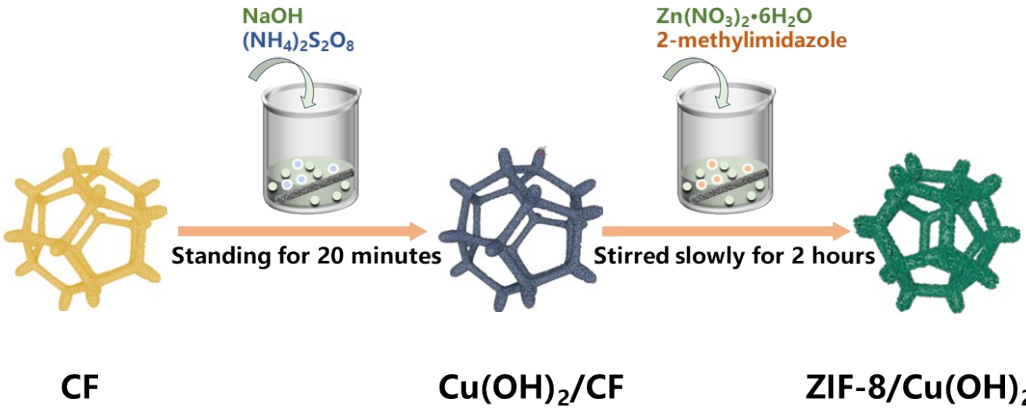

Scheme S1 Schematic illustration of the preparation process of ZIF-8/$Cu(OH)_2$/CF electrocatalyst.

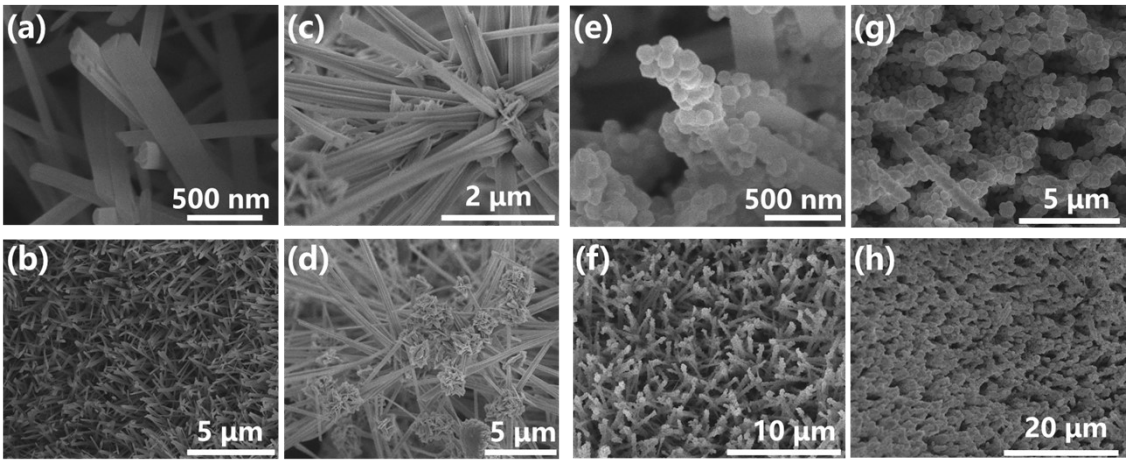

Figure S1 (a-b) SEM images of $Cu(OH)_2$/CF; (c-d) SEM images of ZIF-$8_{0.5}$/$Cu(OH)_2$/CF; (e-f) SEM images of ZIF-$8_{1.5}$/$Cu(OH)_2$/CF; (g-h) SEM images of ZIF-$8_{3.0}$/$Cu(OH)_2$/CF.

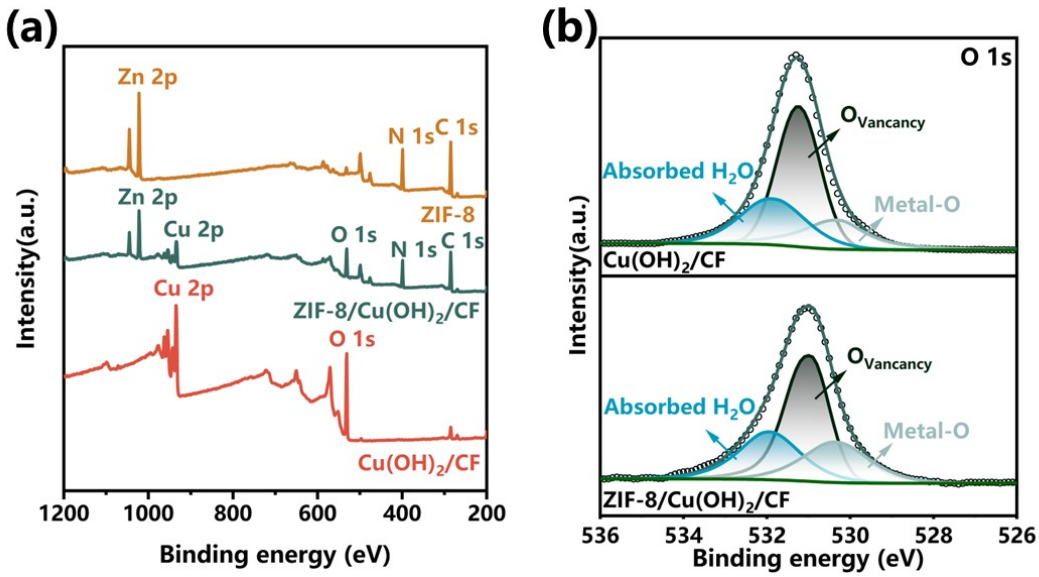

Figure S2 (a) XPS survey spectra of ZIF-8, $Cu(OH)_2$/CF, and ZIF-8/$Cu(OH)_2$/CF; (b) XPS O 1s spectra of ZIF-8 and ZIF-8/$Cu(OH)_2$/CF.

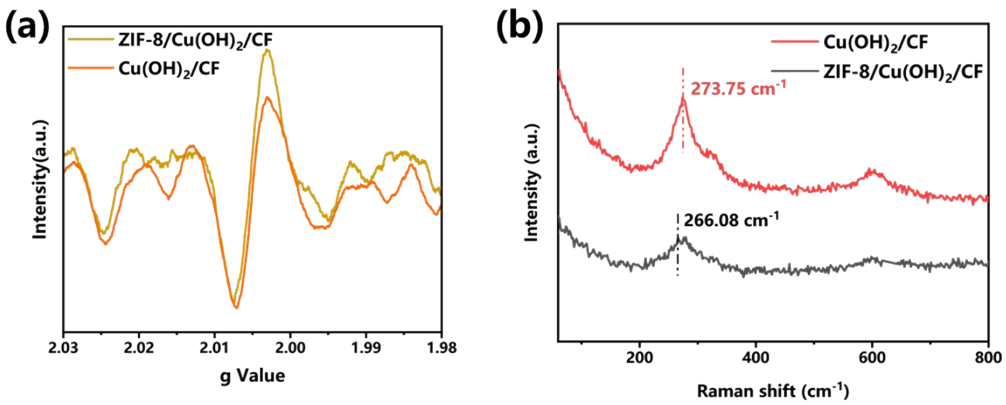

Figure S3 (a) Electron Paramagnetic Resonance (EPR) Spectra of $Cu(OH)_2$/CF and ZIF-8/$Cu(OH)_2$/CF; (b) Raman Spectra of $Cu(OH)_2$/CF and ZIF-8/$Cu(OH)_2$/CF.

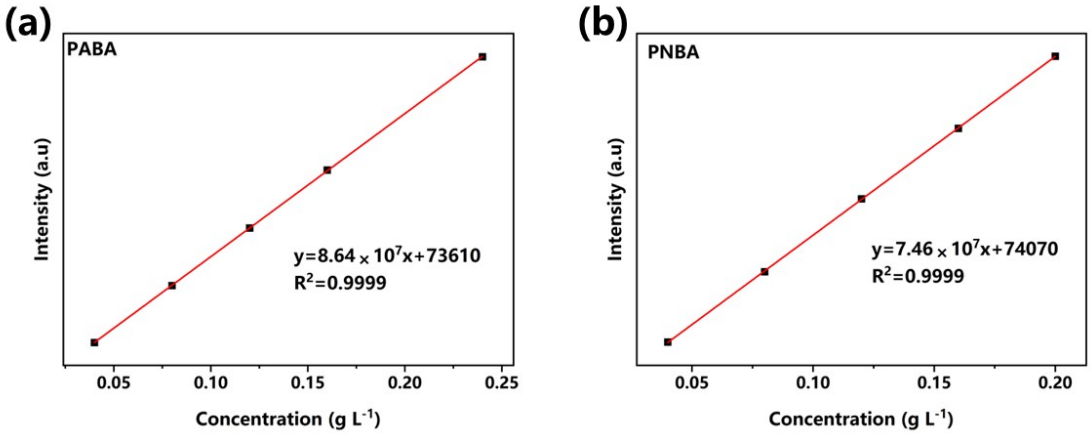

Figure S4 HPLC calibration curves of (a) PABA and (b) PNBA.

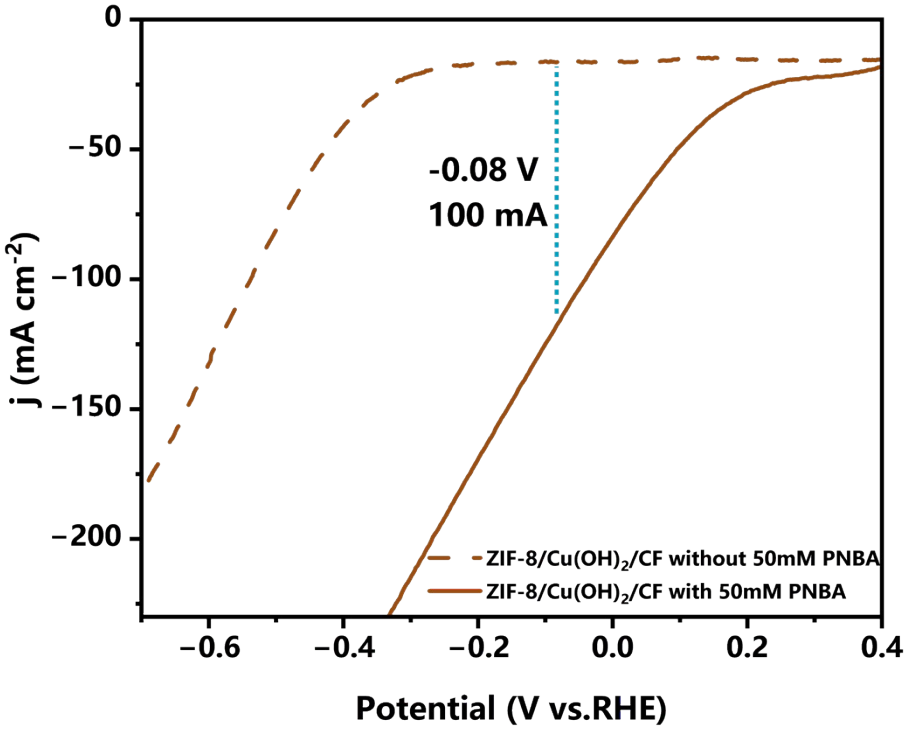

Figure S5 LSV curves of ZIF-8/$Cu(OH)_2$/CF in PBS with and without 50 mM PNBA.

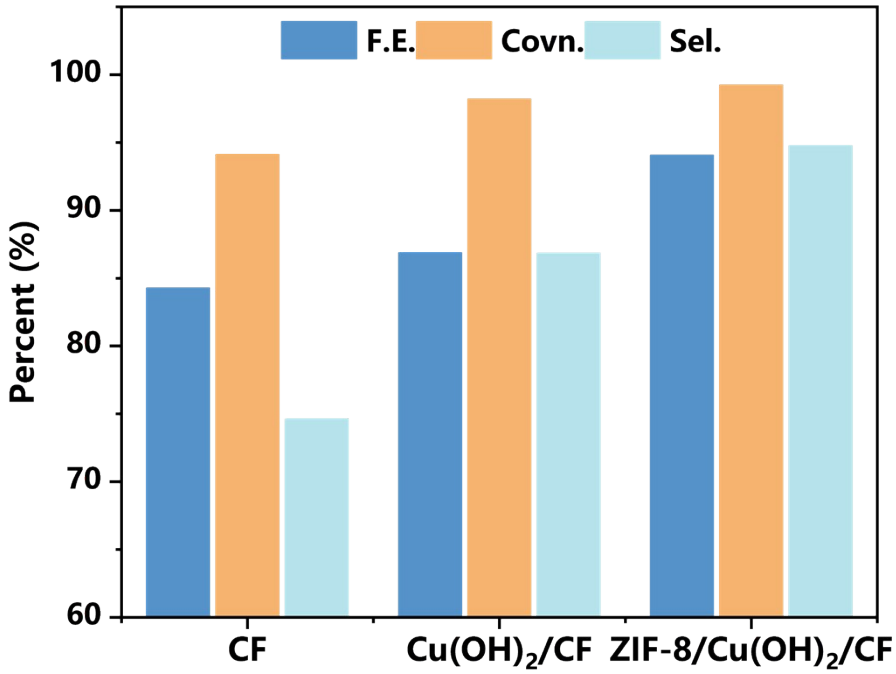

Figure S6 Comparison of Faradaic Efficiency, Conversion, and Selectivity among CF, $Cu(OH)_2$/CF, and ZIF-8/$Cu(OH)_2$/CF.

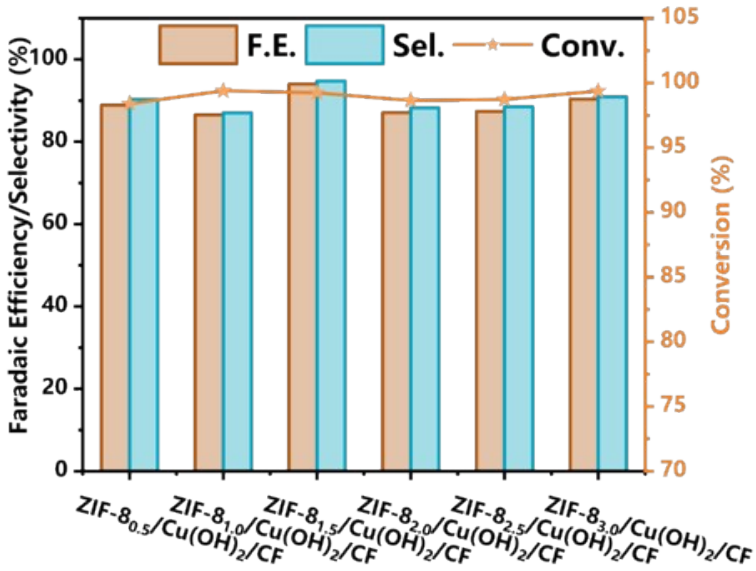

Figure S7 Faradaic efficiency, selectivity, and conversion rate of 50 mM PNBA at -0.345 V (vs. RHE) with varying ZIF-8 concentrations.

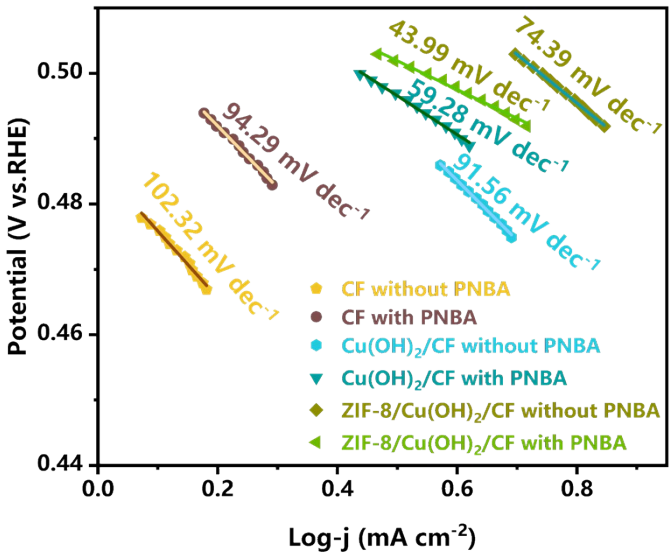

Figure S8 Tafel slopes of CF, $Cu(OH)_2$/CF, and ZIF-8/$Cu(OH)_2$/CF.

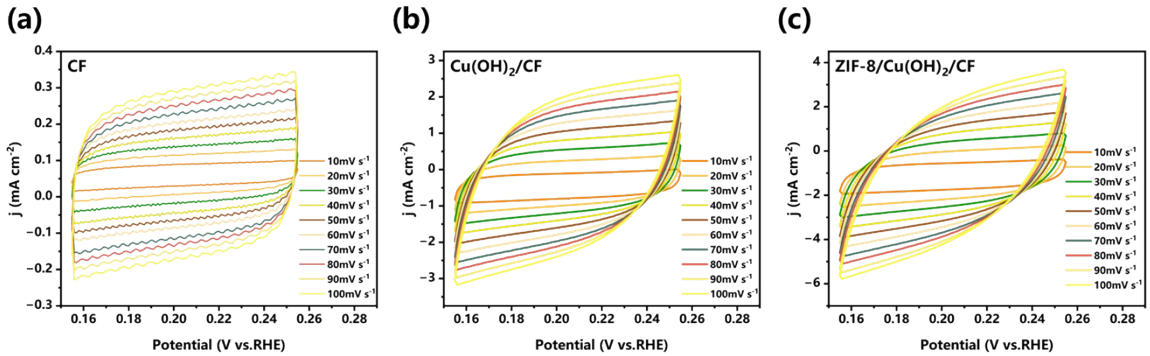

Figure S9 Cyclic voltammograms of (a) CF, (b) $Cu(OH)_2$/CF, and (c) ZIF-8/$Cu(OH)_2$/CF at scan rates ranging from 10 to 100 mV s^{-1}.

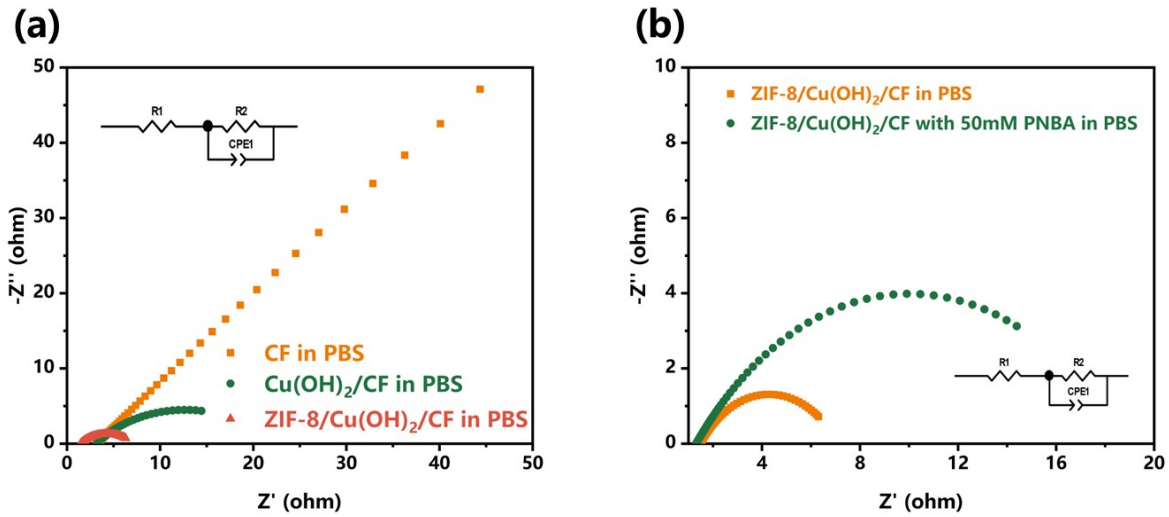

Figure S10 (a) Nyquist plots of ZIF-8/$Cu(OH)_2$/CF in PBS with and without 50 mM PNBA; (b) Comparative Nyquist plots of CF, $Cu(OH)_2$/CF, and ZIF-8/$Cu(OH)_2$/CF in PBS solution, with the inset showing the equivalent circuit model.

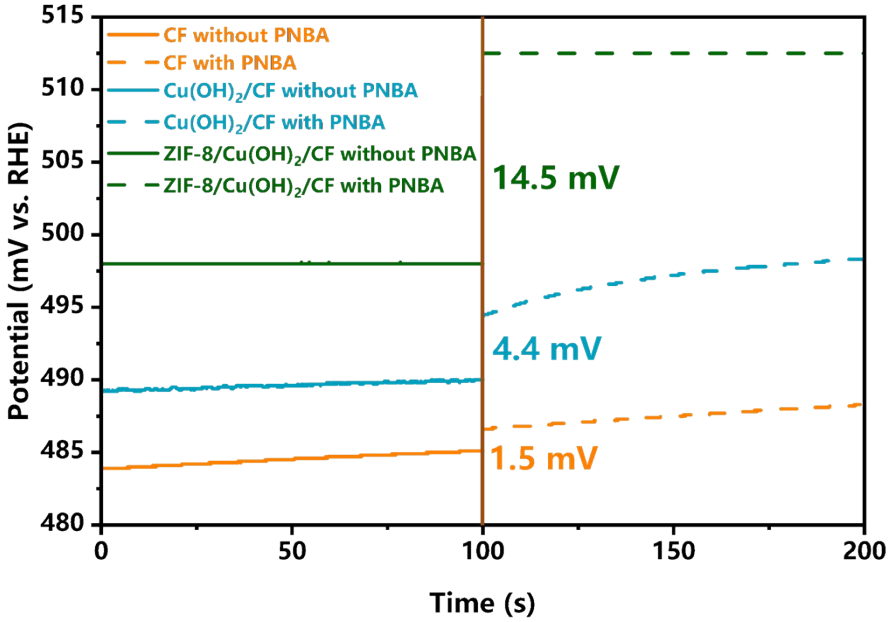

Figure S11 Open Circuit Potential (OCP) Curves of CF, $Cu(OH)_2$/CF, and ZIF-8/$Cu(OH)_2$/CF in PBS with or without 50 mM PNBA.

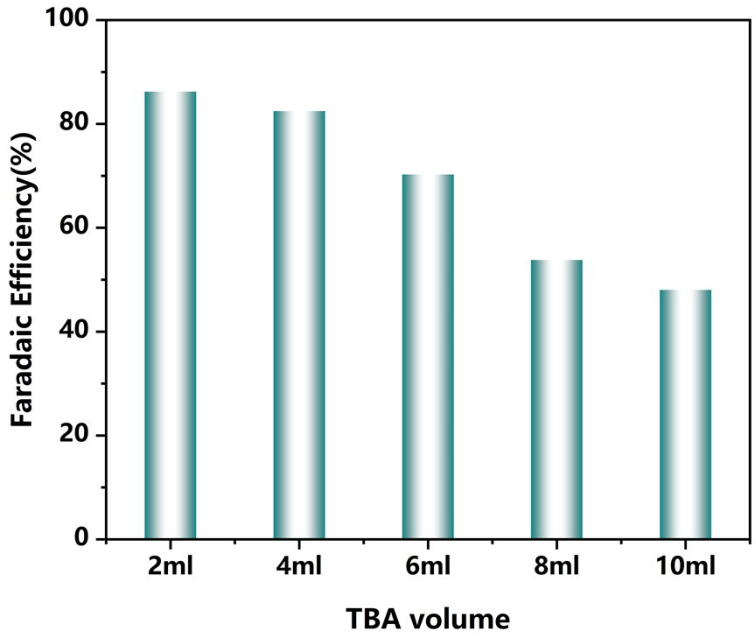

Figure S12 Faradaic Efficiency (FE) of ZIF-8/$Cu(OH)_2$/CF with Different Volumes of TBA Added, Measured at a Potential of -0.345 V (vs. RHE) and a Charge of 1447 C.

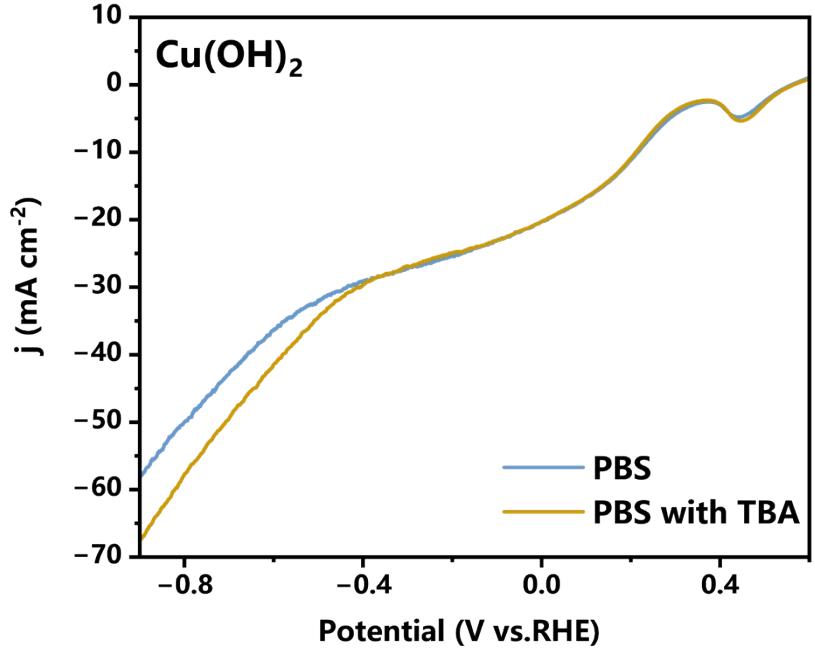

Figure S13 LSV curves of $Cu(OH)_2$ in PBS with and without the addition of TBA.

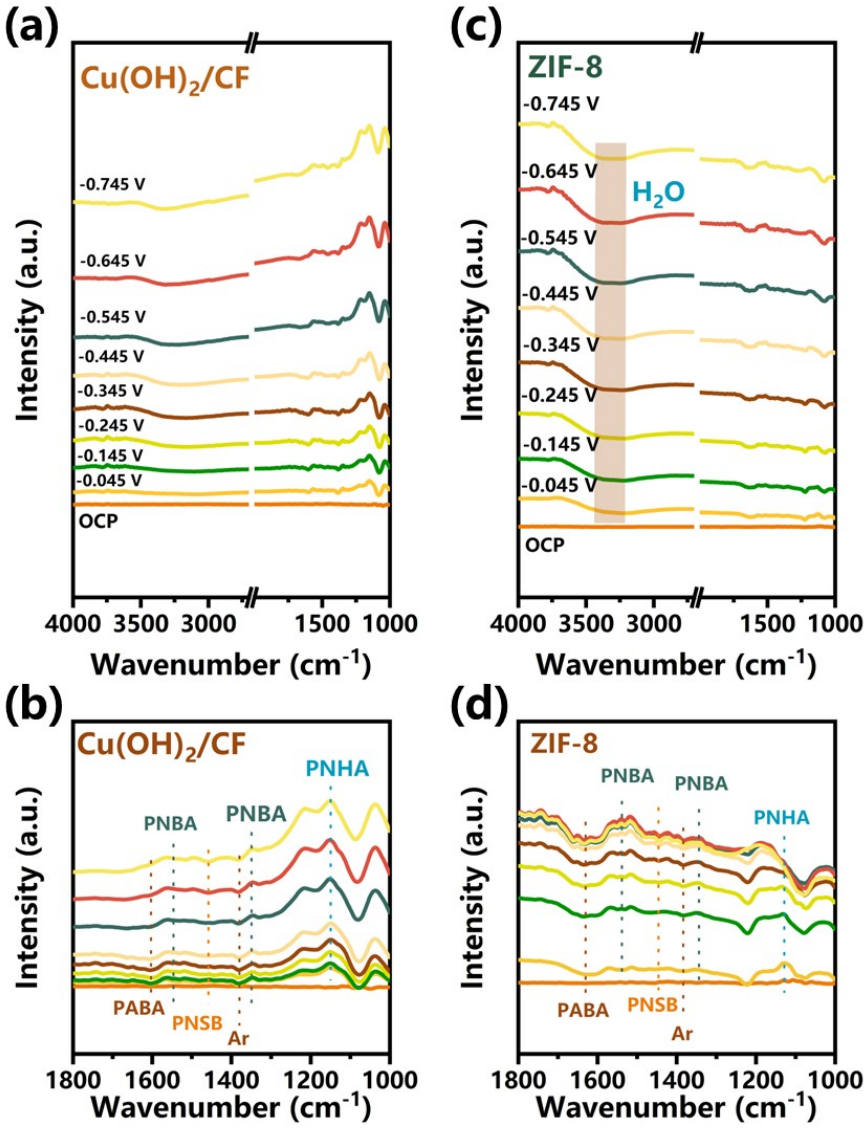

Figure S14 In-situ ATR-FTIR spectra of (a-b) $Cu(OH)_2$; (c-d) ZIF-8 recorded over a potential range from open circuit potentials (OCPs) to −0.745 V vs. reversible hydrogen electrode (RHE). ZIF-8/$Cu(OH)_2$/CF.

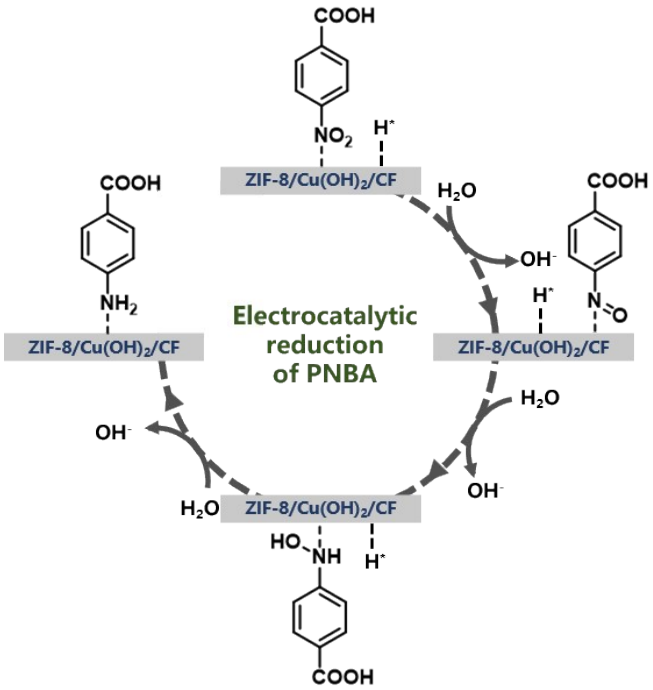

Figure S15 Schematic illustration of the hydrogenation reduction mechanism for the conversion of p-nitrobenzoic acid (PNBA) to p-aminobenzoic acid (PABA).

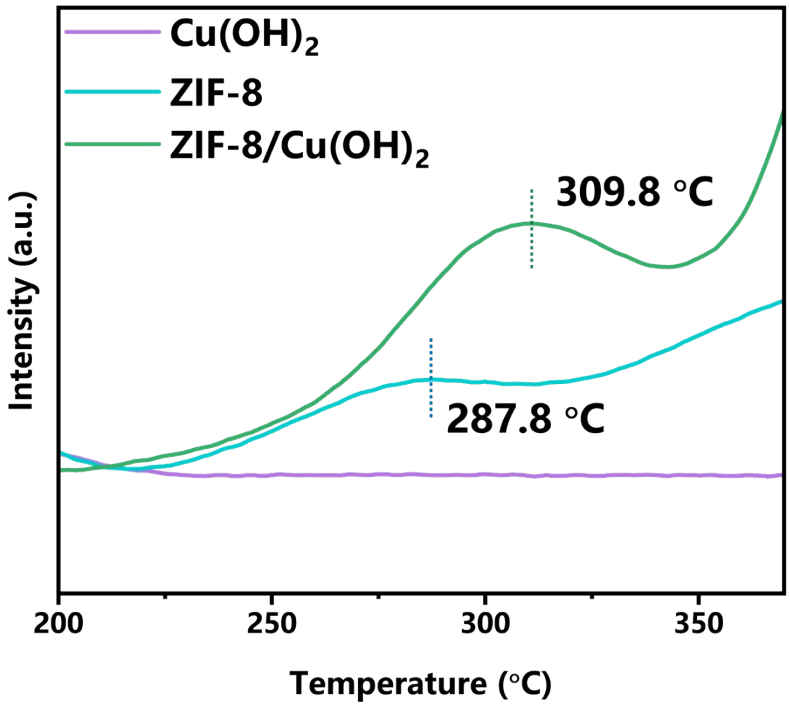

Figure S16 H_2-TPD Profiles of ZIF-8, $Cu(OH)_2$, and ZIF-8/$Cu(OH)_2$.

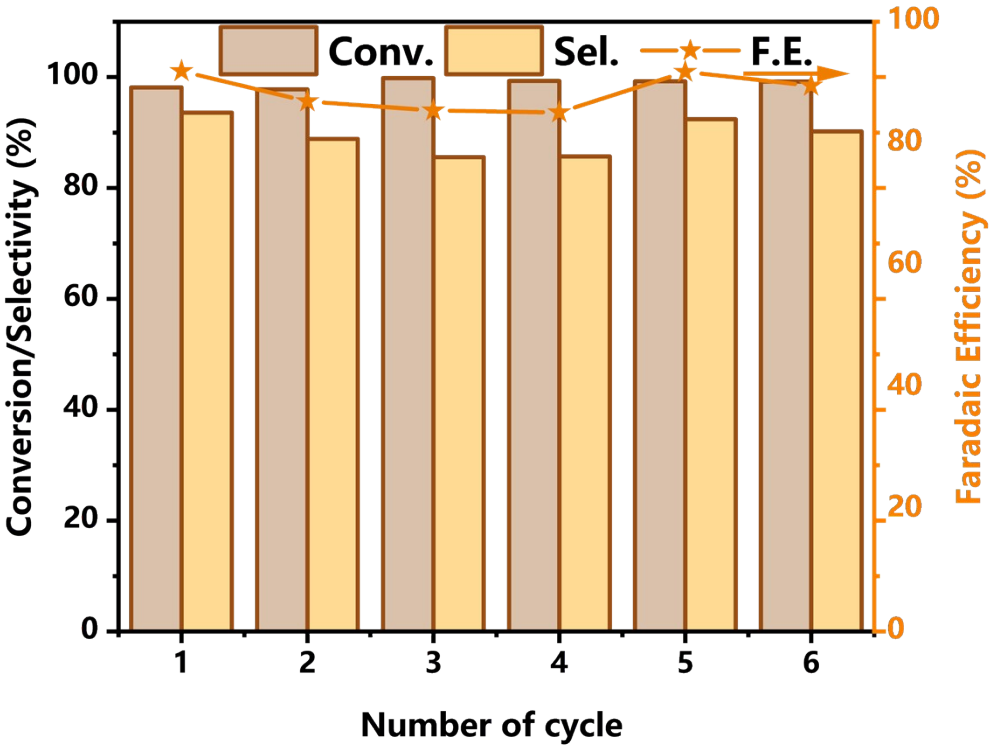

Figure S17 The Faraday efficiency, conversion rate, and selectivity of ZIF-8 after six cycles.

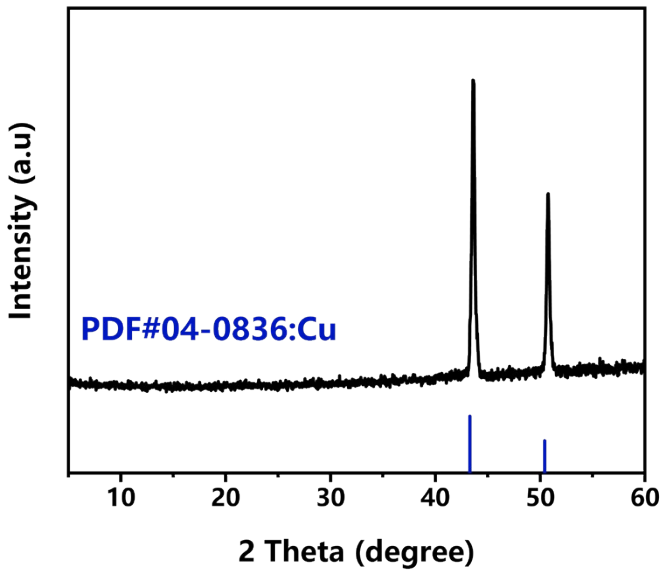

Figure S18 XRD pattern of the ZIF-8/$Cu(OH)_2$/CF composite after reaction.

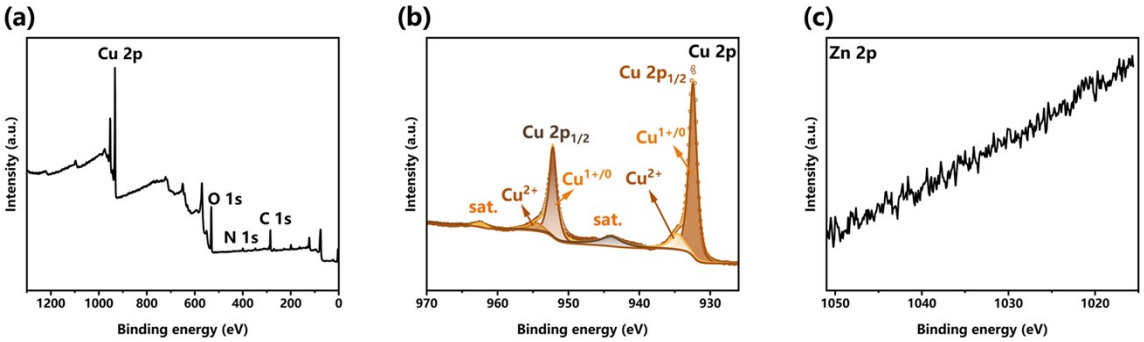

Figure S19 (a) XPS survey spectrum, (b) high-resolution Cu 2p XPS spectrum, and (c) high-resolution Zn 2p XPS spectrum of the ZIF-8/$Cu(OH)_2$/CF composite after reaction.

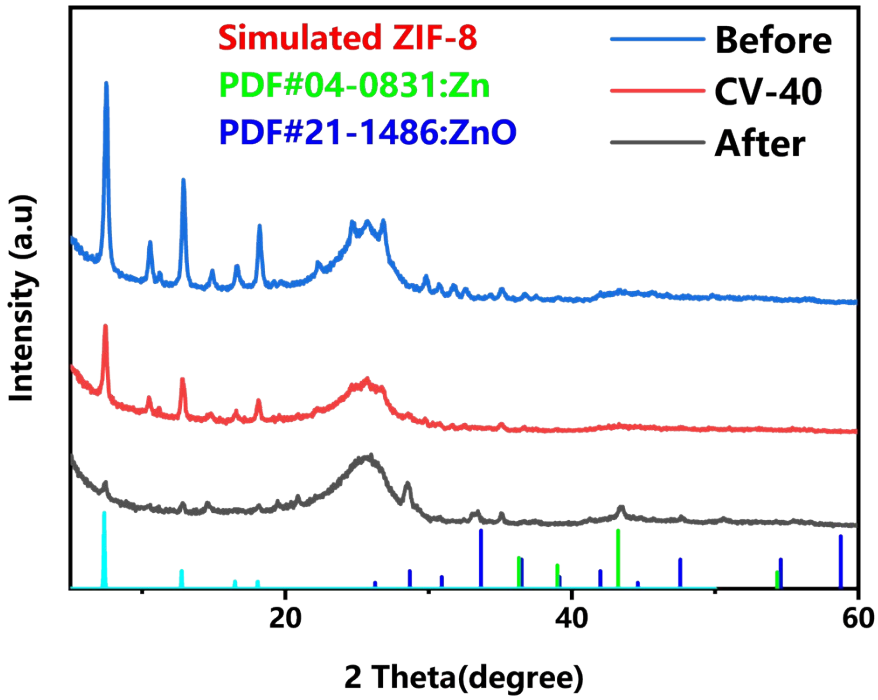

Figure S20 XRD patterns of the ZIF-8 material before 40 cycles of cyclic voltammetry (CV) scanning and after reaction.

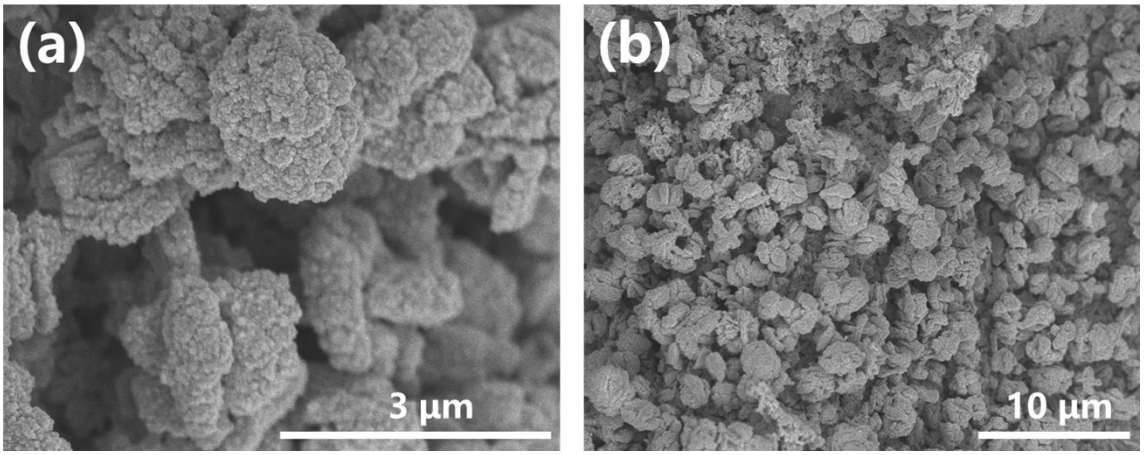

Figure S21 (a-b) SEM Image of ZIF-8/$Cu(OH)_2$/CF After Reaction.

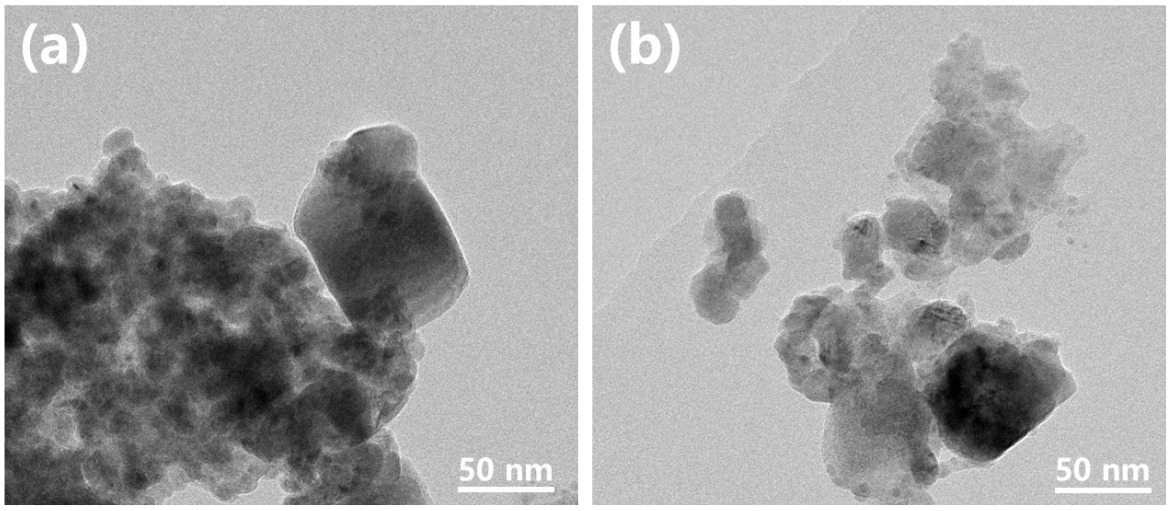

Figure S22 (a-b) TEM Image of ZIF-8/$Cu(OH)_2$/CF after reaction.

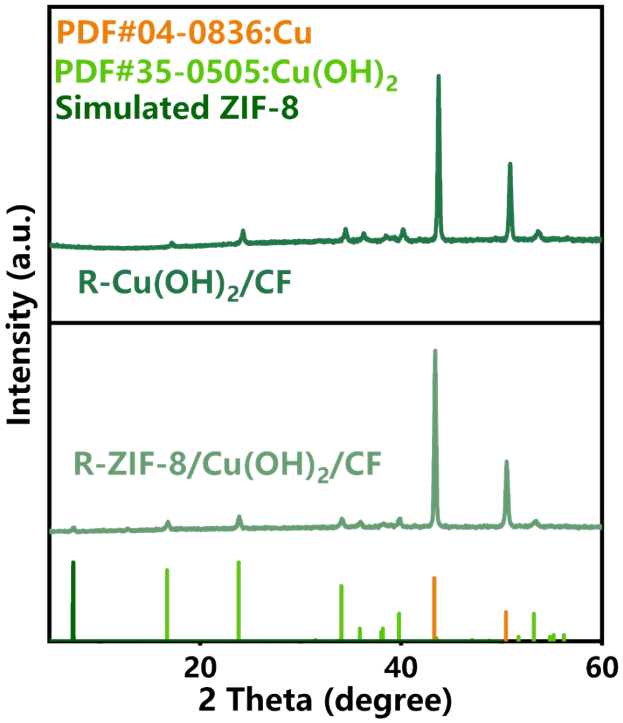

Figure S23 X-ray diffraction (XRD) patterns of the resynthesized $Cu(OH)_2$/CF material and ZIF-8/$Cu(OH)_2$/CF composite.

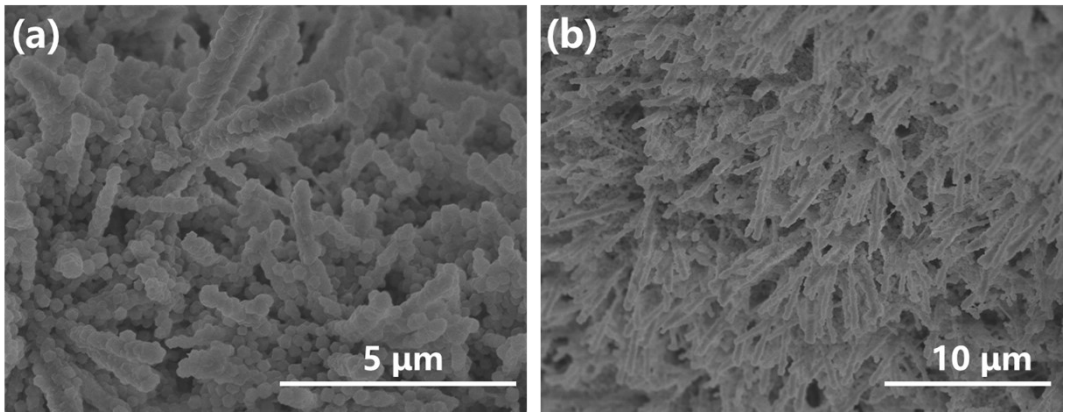

Figure S24 (a-b)SEM Image of the Resynthesized ZIF-8/$Cu(OH)_2$/CF composite after reaction.

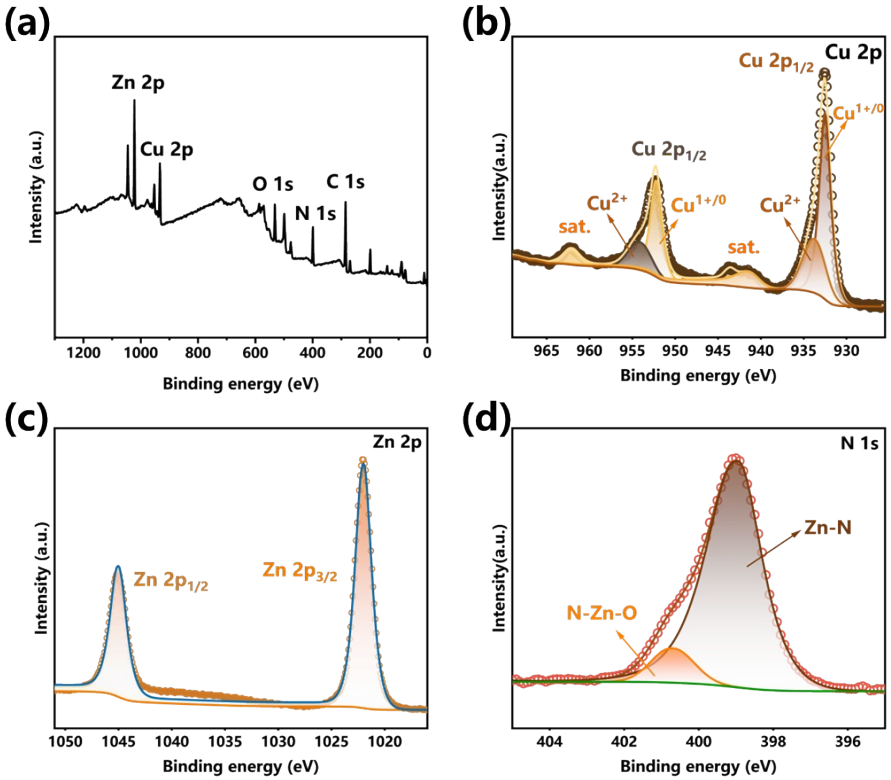

Figure S25 XPS Spectra of the Resynthesized ZIF-8/$Cu(OH)_2$/CF Material, (a) XPS survey spectra;(b)Cu 2p; (c) Zn 2p; (d) N 1s.

Table S1 Elemental composition ratios of ZIF-8/$Cu(OH)_2$/CF.

Element	Atomic Fraction(%)
C	29.64
N	14.65
O	31.88
Cu	21.02
Zn	2.80